Electronic Supplementary Material (ESI) for Lab on a Chip.
This journal is © The Royal Society of Chemistry 2019

Supporting Information

Gradient-sized control of tumour spheroids on a single chip

Guocheng Fang[a], Hongxu Lu[a], Andrew Law[b], David Gallego-Ortega[b,c], Dayong Jin[a,d] and Gungun Lin[a]*

[a]Institute for Biomedical Materials and Devices, Faculty of Science, The University of Technology Sydney, Ultimo, New South Wales 2007, Australia.
[b] Garvan Institute of Medical Research, 384 Victoria Street, Darlinghurst NSW 2010, Australia
[c] St. Vincent's Clinical School, Faculty of Medicine, University of New South Wales Sydney. Kensington, New South Wales 2052. Australia
[d] UTS-SUStech Joint Research Centre for Biomedical Materials & Devices, Department of Biomedical Engineering, Southern University of Science and Technology, Shenzhen, China

** E-mail: Hongxu.Lu@uts.edu.au*

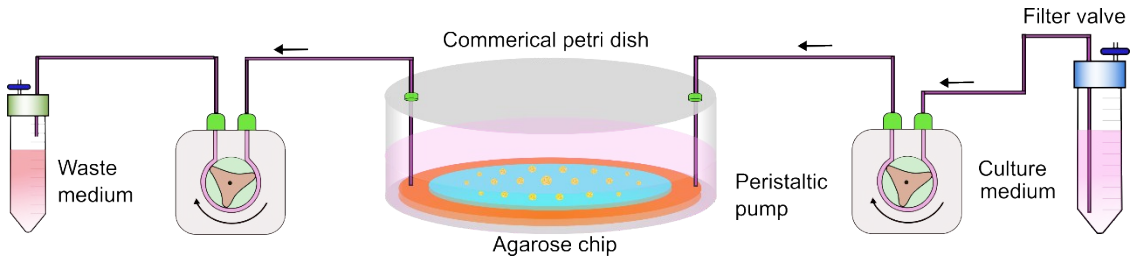

Fig. S1. Schematic of the dynamic irrigation culture system integrated with the peristaltic pump and commercial cell culture plate.

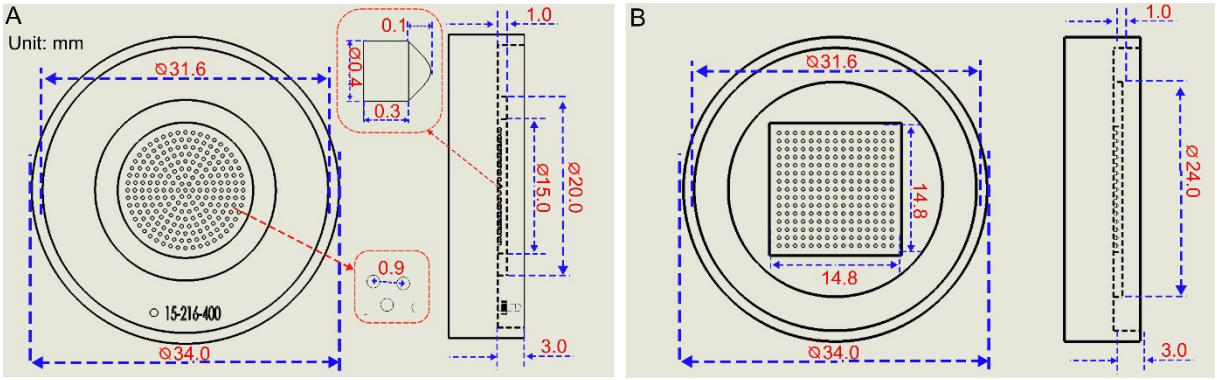

Fig. S2. Engineering drawings of the round-array mould and the square-array mould.

The micropillars' height is 300 μm, the diameter is 400 μm and the conical top is 100 μm in height. The distance between each micropillars is 0.9 mm. There are 217 and 225 microwells on the round-array chip and the square-array chip, respectively. The thickness of the agarose chip is designed to be less than 3 mm.

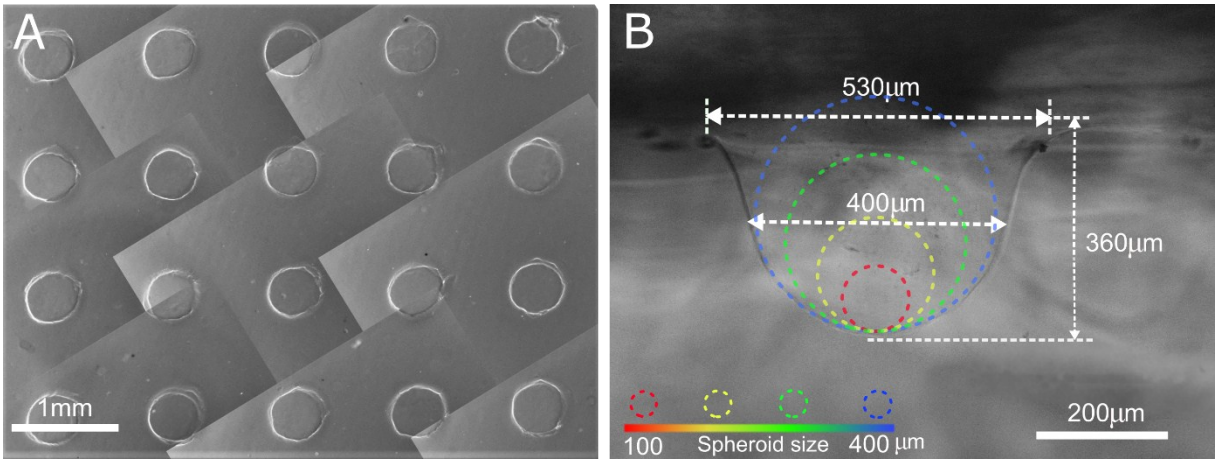

Fig. S3. Top-view image of the microwells. (B) Side-view image of the microwells.

As shown in **Fig.S3 (A)**, the microwells show good sphericity. After several week's immersion in the culture medium, the sphericity does not change a lot. Side-view image of the microwell is illustrated in **Fig.S3 (B)**. The microwell shows a conical shape with a relatively flat bottom. The diameter of the top opening is ~530 μm, although the diameter of the mould pillar is designed as 400 μm. The height is about ~360 μm. In the middle height, the diameter is ~400 μm. With this dimension design, the microwell can allow the spheroids up to 400 μm. The iridescent model shown in **FigS3. (B)** represents the spheroid size.

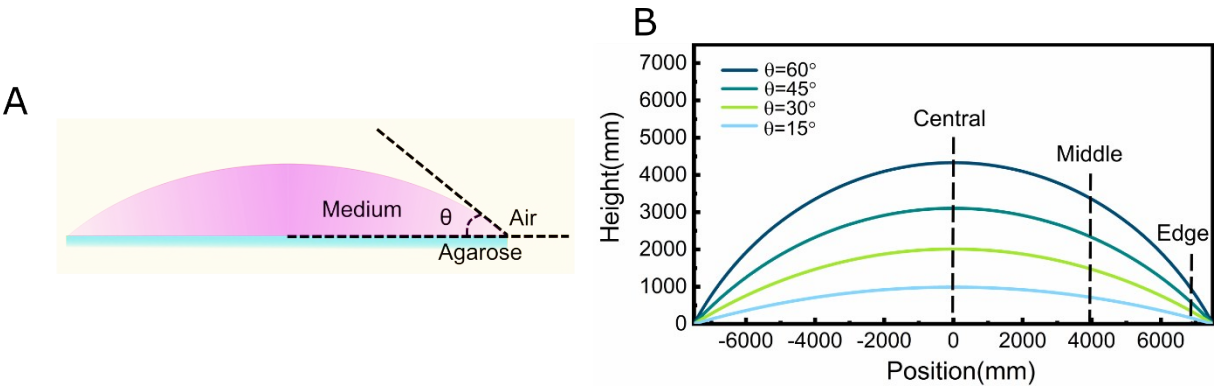

Fig. S4. (A) Schematic of the contact angle (loaded medium volume) at the air-medium-agarose barrier area. (B) The relationship of liquid height and position under different contact angle situation based on the hemisphere-shaped dome model.

Table S1. Theoretical simulation of the liquid height at different positions under different contact angle (Value in blanket is the ratio of central height to middle height & edge height).

	15°	30°	45°	60°
Central	0.132	0.268	0.414	0.577
Middle (50%)	0.099 (1.33)	0.204 (1.31)	0.323 (1.28)	0.464 (1.24)
Edge (85%)	0.037 (3.57)	0.078 (3.44)	0.130 (3.18)	0.204 (2.83)

Due to the complex force interactions at the air-medium-agarose barrier area, the contact angle cannot be preciously calculated. Here, we assumed that the medium volume loaded on the chip

could change the contact angle and used the hemisphere-shaped models to analyse the contact angle effect. According to **Fig. S4B** and **Table S1**, it indicates that when the contact angle changed from 15º to 60º, the height difference ratio (central height/edge height) changes slightly, which remains ~3 folds. Here, we define the size modulation ability is proportional to the height difference ratio. Accordingly, we could conclude that the medium volume and the contact angle had an ignorable influence on the modulation ability of the liquid dome in this study.

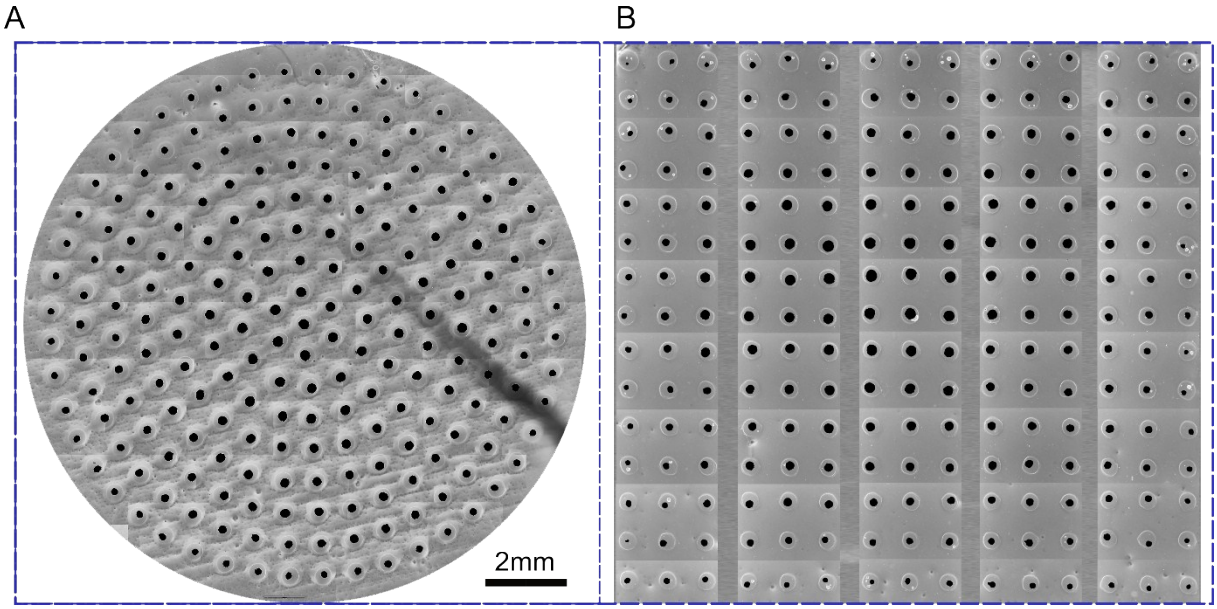

Fig. S5. Raw data of the spheroids on chip. (A) Spheroids on round-array chip processed by ImageJ. (B). Spheroids on square-array chip processed by ImageJ

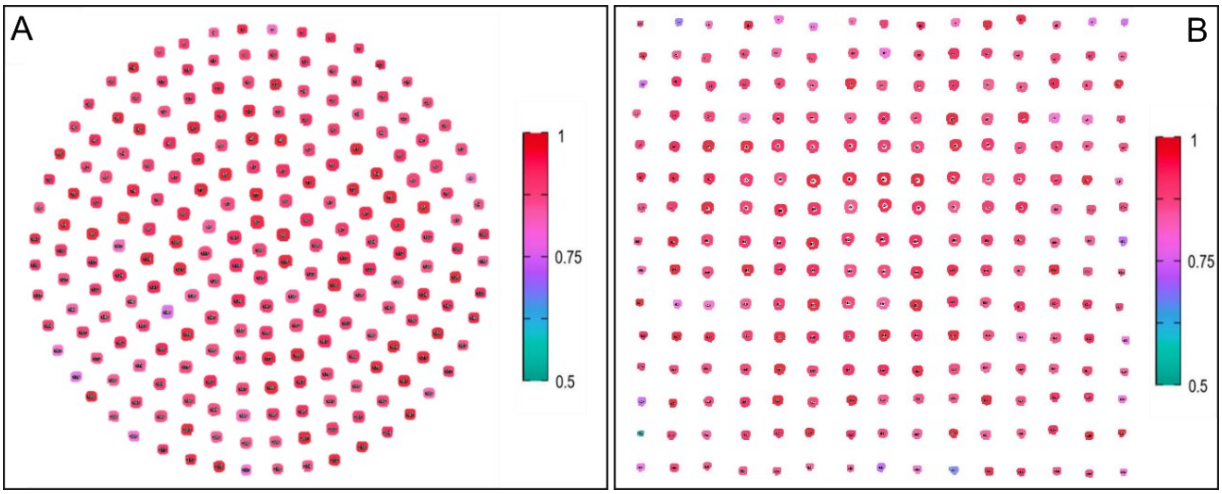

Fig. S6. Roundness of each spheroid (1-day-old) measured by ImageJ.

The spheroids on the chip had high roundness as shown in **Fig S6**, most of which were around 0.9. This indicates that the roundness of the spheroid was independent with the size at the initial growing stage.

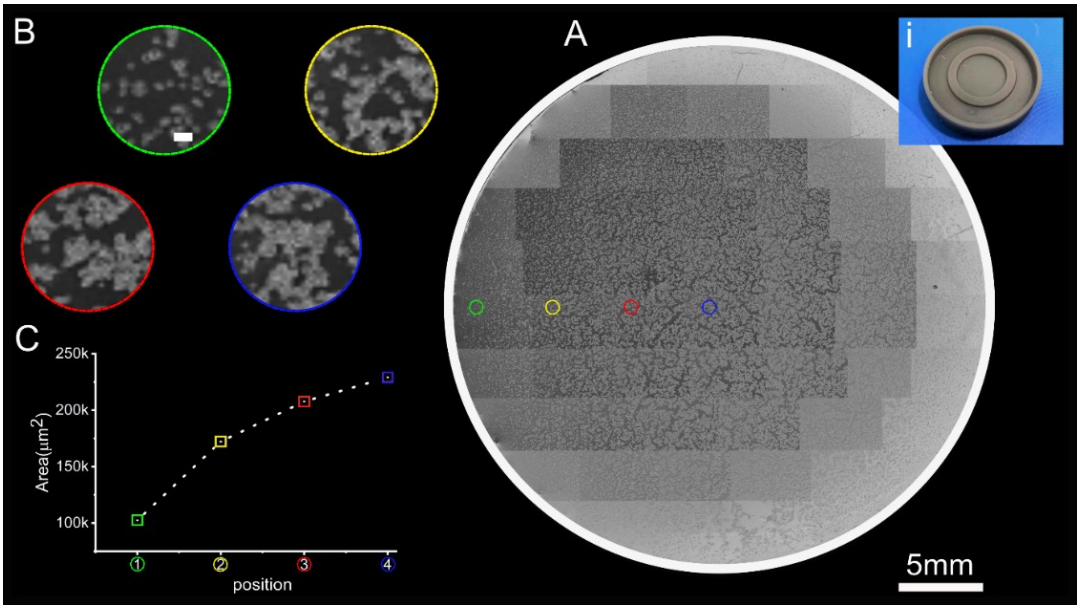

Fig. S7. No-micropillar mould for the investigation of the cell sedimentation distribution. (A) Image of the cell distribution after the sedimentation. i) Inset is the mould without micropillars. (B) Enlarged view of the four selected spots along the diameter (Scale bar:100 μm). (C) Relationship of the cell area and position of the coloured circles.

To further prove the mechanism of the liquid dome, a chip without the microwells was fabricated via a mould without the micropillars. After cell suspension loading and sedimentation, the cells were distributed on the whole surface. It could be seen that the distribution of the cells indeed followed the central-edge rule. Images in the coloured circles show the enlarged views of the cells in four different places. (Scale bar:100μm) By analysing the cell area in the circles, an obvious increase was seen from the edge to the central. The images were captured before pricking the liquid dome.

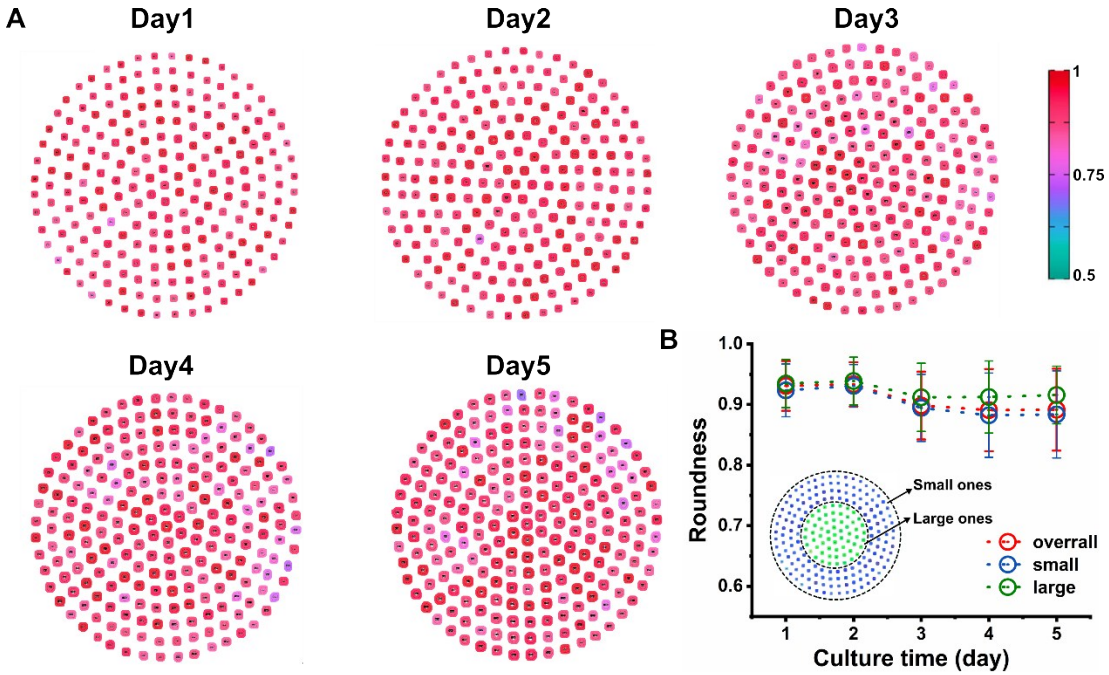

Fig. S8. (A) Roundness profile of the MCF-7 spheroids on the chip for 5 days. (B). Roundness change versus culture time.

The roundness change of the spheroids on the round chip was tracked for 5 days. According to **Fig.S8**, it was seen that the overall sphericity was around 0.92. On the second day, the overall roundness slightly increased, which was followed by a drop on the third day. Then the roundness stayed at 0.90 on day 4 and 5. After 5-day's culture, although the roundness of some spheroids became worse to around 0.75, most spheroids had high sphericity (remaining at around 0.9).

To illustrate the roundness difference among the different-sized spheroids, we defined the spheroids at the edge area as the small ones and the spheroids at the central area as the large ones, as shown in **Fig. S8**. We could see that there was little difference in roundness between small and large spheroids at day 1. Specifically, after several days' culture, the roundness of the large spheroids was higher than that of the small spheroids. From the roundness profile, we could see that spheroids with lower roundness were likely distributed at the edge area. This indicated that the spheroids with large size have more stability than that with small size.

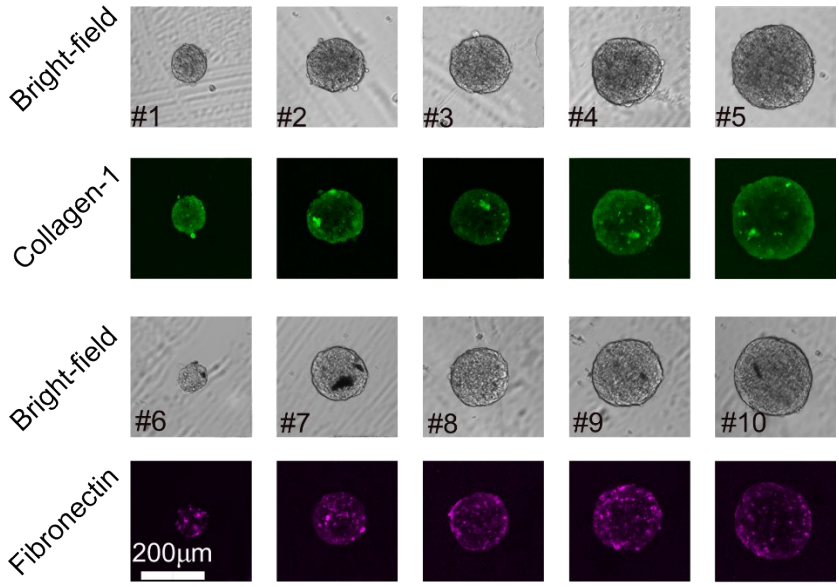

Fig. S9. Collagen type I and fibronectin distribution in the MCF-7 spheroids.

We investigated the ECM molecules, including collagen type I and fibronectin, in the MCF-7 spheroids formed on this chip. The spheroids were fixed with 4% paraformaldehyde, permeated with 1% Triton X-100, and stained with antibodies against collagen type I and fibronectin, respectively. Then fluorescent second antibodies were applied to the spheroids. As shown in **Fig. S9**, both collagen type I and fibronectin can be observed in the spheroids. There is no noticeable difference among spheroids of different sizes. It coincides with the literature[1] that a variety of ECM molecules can be found in the spheroids including collagen type I, fibronectin, laminin et al.

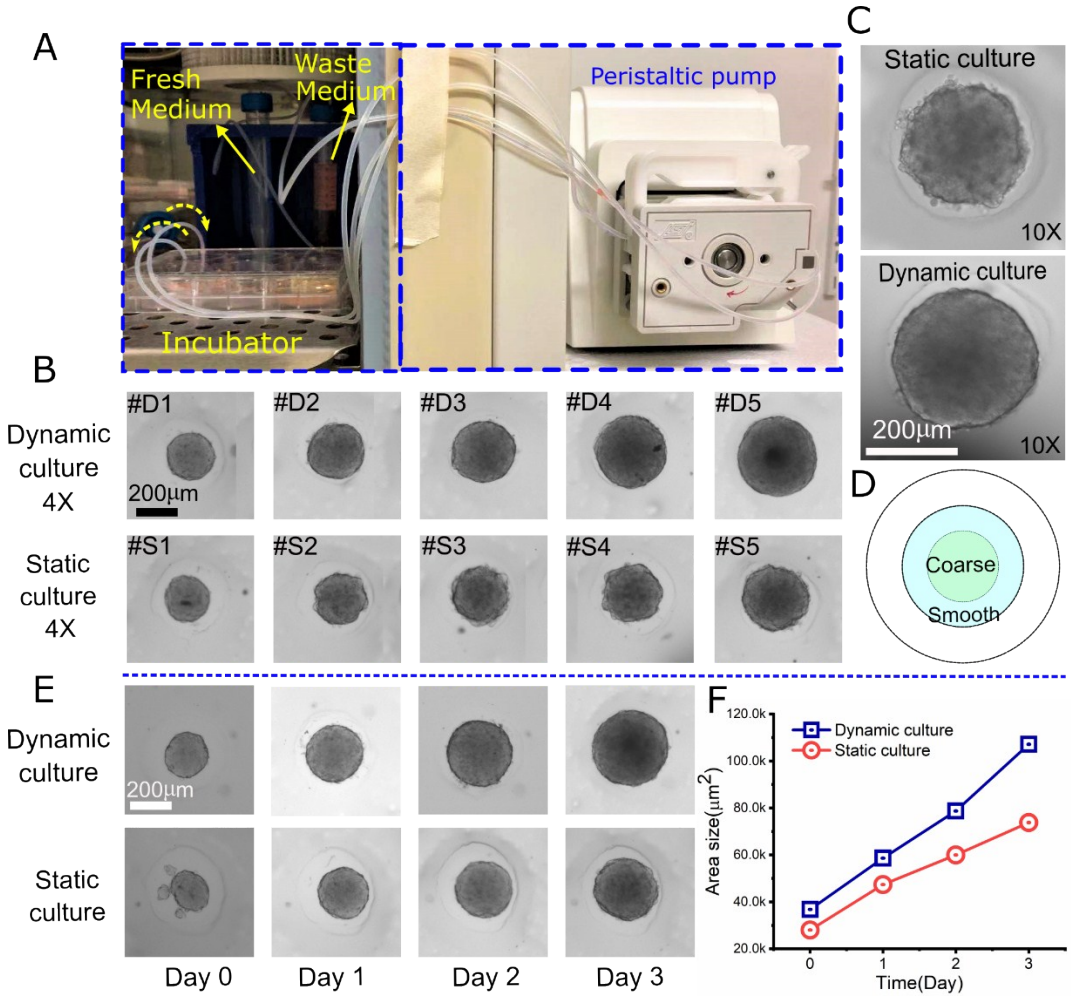

Fig. S10. (A) Experimental setup of the microfluidic dynamic culture. (B) Comparison of the spheroids with dynamic culture and static culture observed with a 4X objective lens. (C) Surface of the spheroids with dynamic culture and static culture. (D) On-chip distribution of the spheroids with coarse and smooth surface under static culture. (E) Growth of the spheroids with dynamic culture and static culture. (F) Growth curve of the spheroids with dynamic culture and static culture.

To characterize the difference of perfusion (dynamic) culture and the static culture, we added the microfluidic perfusion unit. The microfluidic perfusion setup, as shown in **Fig. S10(A),** consisted of a peristaltic pump, a tube containing fresh medium, a tubing containing waste medium, the chip in the 6-well cultural plate and the silicon tube. The flow rate was set as 50 uL/h, which could offer 1 mL fresh medium for 1 day. The medium of the control group was

changed with 2 mL every 2 days. Interestingly, we found that the spheroids with dynamic perfusion had a smoother surface, as shown in **Fig. S10 (B) &(C)**. Distribution of the smooth and coarse spheroids under static culture is shown in **Fig. S10 (D)**. Without the perfusion, the spheroids at the central area tended to have a coarse surface, and those at the edge prefer a smooth surface. We supposed that the central area had fast nutrition consume and metabolic waste accumulation under the static culture. When the perfusion was applied, the nutrition had a homogeneous distribution and the metabolic waste could be cleaned up in time. We also compared the difference in growth rate. **Fig. S10 (E)** shows the growth of two spheroids with the same position on the chip. According to **Fig. S10 (F)**, the spheroids with perfusion had an increasing growth rate. However, the spheroid without perfusion showed a decreasing growth rate. This indicates that the microfluidic unit could offer a better living environment for the spheroids.

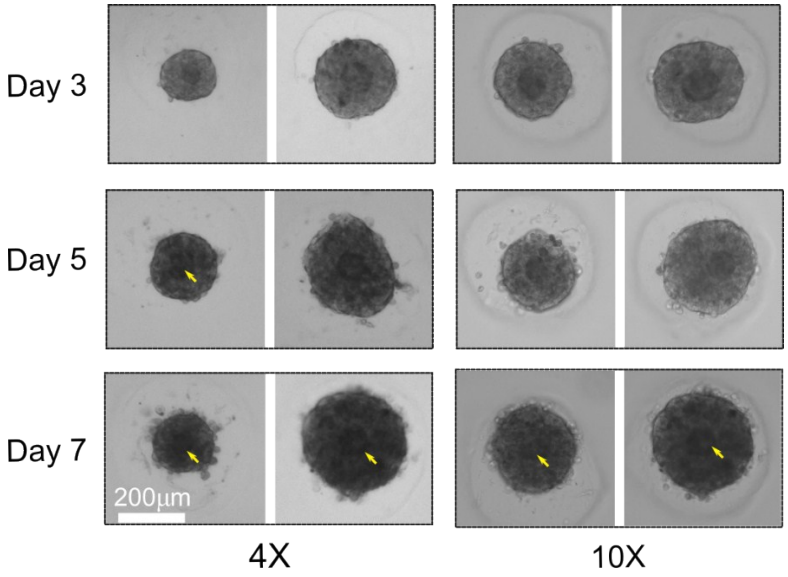

Fig. S11. Spheroids formed by the co-culture of MCF-7 and fibroblasts. (Scale bar:200 μm).

To test the stability of the co-culture model, we prolonged the culture of spheroids for up to 1 week. Although it was a little difficult to track these two kinds of cells with this dye, it was

easier to distinguish the fibroblast core and MCF-7 shell. As shown in **Fig.S11**, the core could be observed at day 3. At day 5, although the spheroid density became larger, the fibroblast could also be seen in the central area. At day 7, the spheroid density continued to be larger, and the fibroblast core was hard to be observed in most spheroids. However, in some spheroids, we could still observe the core-shell structure. This indicates that the fibroblast core-MCF-7 shell spheroid model can be stable for up to 1 week.

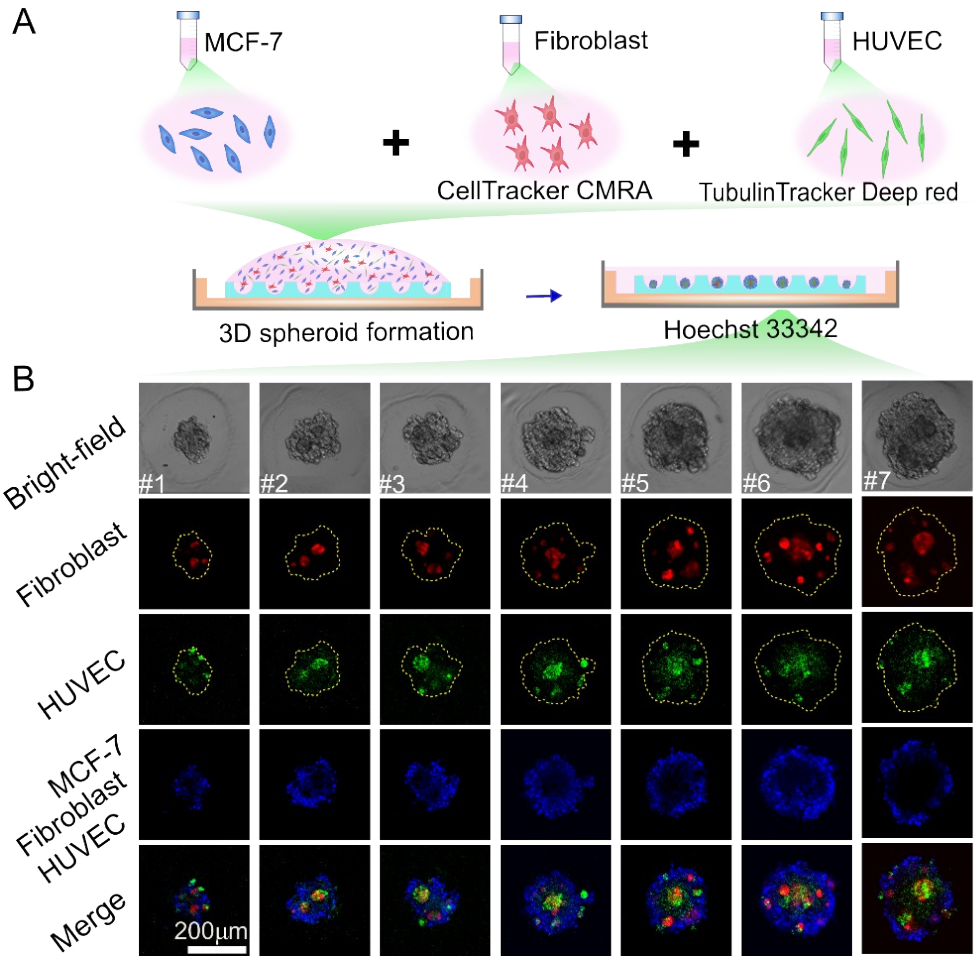

Fig. S12. (A) Schematic of the triple coculture of MCF-7, fibroblasts and HUVEC. (B). Gradient-sized spheroid formed by MCF-7, fibroblast (red fluorescence) and HUVEC (green fluorescence). (Scale bar:200 μm).

To better mimic the tumor microenvironment, we introduced the Human Umbilical Vein Endothelial Cells (HUVEC) into the spheroids and co-cultured these three types of cells, as shown in **Fig. S12 (A)**. HUVEC are commonly used for the modelling angiogenesis in 3D models. The co-culture of HUVEC with tumor cells and fibroblasts could help to research the crosstalk between tumor cells and endothelial cells, which is critical for the new blood formation, known as the angiogenesis.

Here, the fibroblasts were stained red with CellTracker CMRA, HUVEC were stained greed with Tubulin Tracker Deep red, as shown in **Fig. S12(A)**. Then the MCF-7, fibroblast and HUVEC were mixed at a ratio of 5:1:1 and seeded on the chip followed the process in the manuscript. After 1 day's culture, the gradient-sized triple-cell spheroids were formed on this chip, as shown in **Fig.S12 (B)**. It could be seen that the roundness of the spheroids had a slight decrease when the HUVEC were added, especially for the small spheroids. The central tendency of the fibroblasts changed a little bit. More fibroblast cores occurred in the spheroids; however, the central tendency could also be seen in some large spheroids. Another interesting thing is that the green fluorescence seemed to overlap well with the red fluorescence, indicating that the HUVEC preferred to stay together with the fibroblasts.

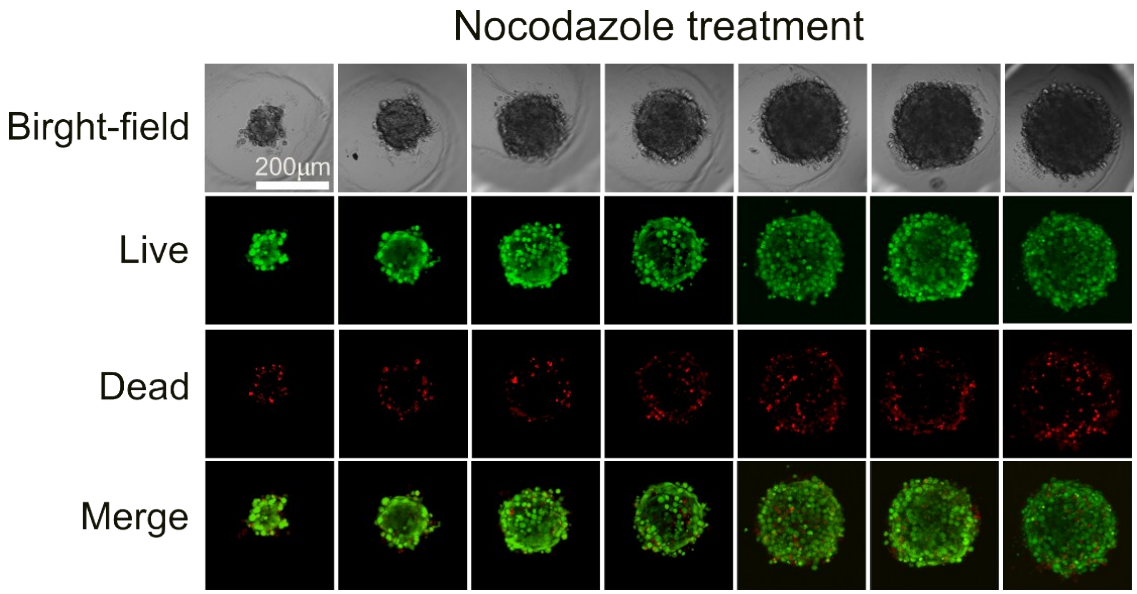

Fig. S13. Gradient-sized spheroids treated with Nocodazole (3.5μM, 72h).

On the recommended concentration, the spheroids gave less response to Nocodazole, although the spheroids seemed to get turbid in the bright-field images. The viability in different-sized spheroids was relatively high.

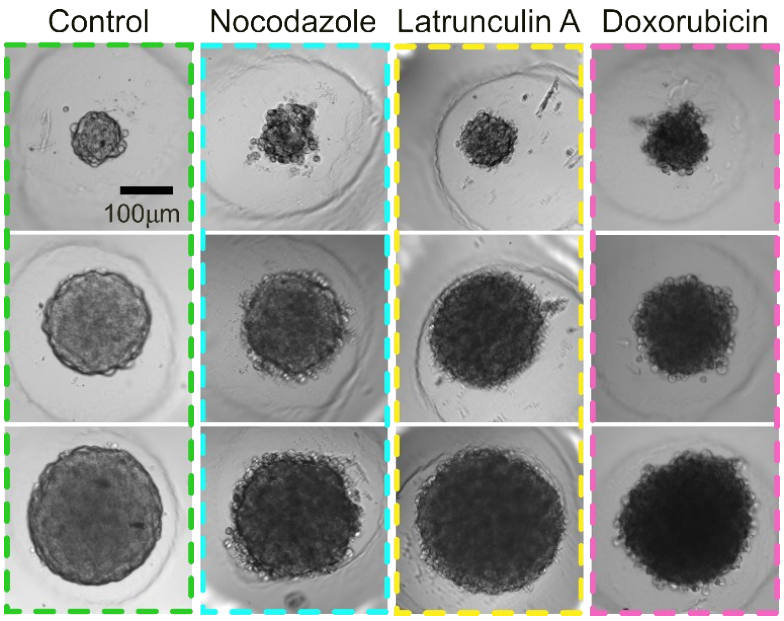

Fig. S14. Bright-field images of the spheroids treated with Nocodazole, Latrunculin A and DOX for 72h.

After the drug treatment, all the spheroids became turbid compared with the control group. In the control group, the spheroids had clear and tight edge. In the Nocodazole group, although some cells became round on the surface and dropped off, a clear edge could still be observed. In the Latrunculin A group, the different-sized spheroids became turbid and the edge line became indiscernible. But the cell remained in the spheroids with less cells dropping off. In the DOX group, the spheroids became more turbid and some cells became round with more cells dropping off. The edge line was also indiscernible.

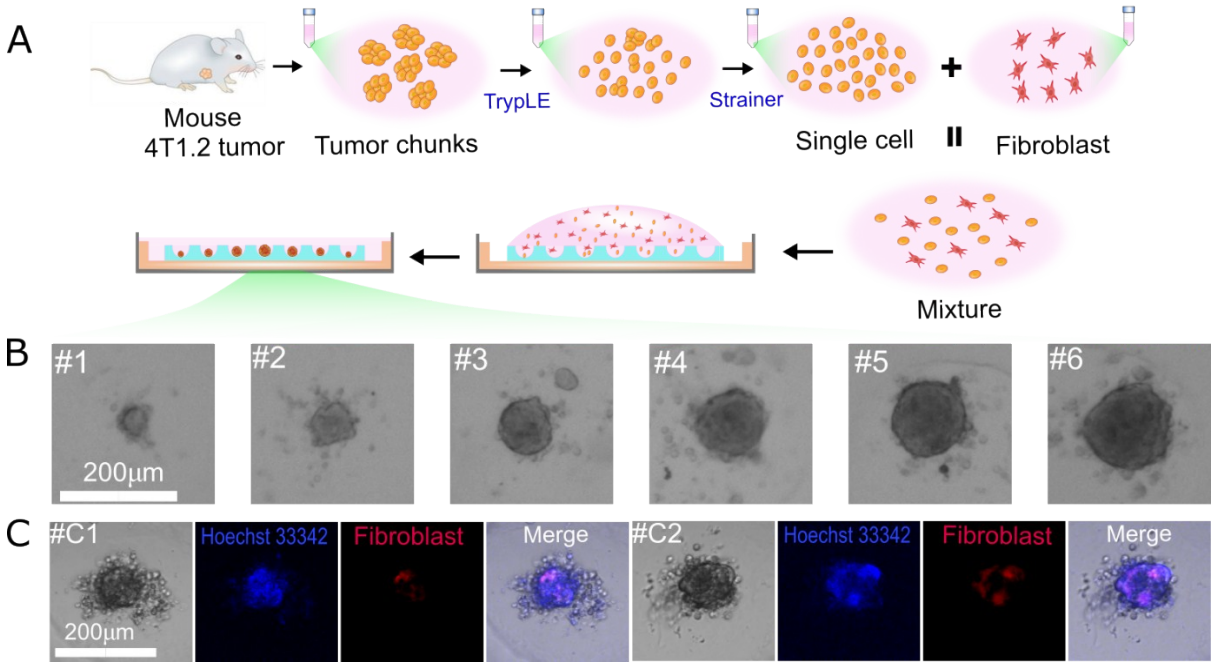

Fig. S15. (A) Schematic of the spheroids formation process on this chip with mouse 4T1 tumor cells and fibroblasts. (B) Mouse 4T1.2-fibroblast spheroids with gradient size formed on the chip. (C) Distribution of the mouse 4T1.2 cells and fibroblast in the spheroids. Fibroblasts were stained red with CellTracker CMRA Orange, and the whole spheroids were stained blue with Hoechst 33342.

To better illustrate the capacity of this method, we used the mouse 4T1.2 tissue as a model of the patient tumor sample to fabricate the gradient-sized spheroids on this chip. As shown in **Fig. S15(A)**, at first, the mouse 4T1.2 tumor was removed and chopped into small chunks. Then

the chunks were treated with TrypLE™ Express (Thermo Fisher, Australia) for 10 mins to dissociate into single cells. Next, the small chunks were removed by a cell strainer with 200 μm pore size. Then the single cells were mixed with fibroblasts at a ratio of 3:1, which followed the seeding process in the Materials and Methods. As shown in **Fig. S15(B)**, the gradient-sized spheroids could be formed on this chip. Compared to the MCF-7 (cell line), some cells scattered around the spheroids. To investigate the distribution of the 4T1.2 tumor and fibroblasts in spheroids, we stained the fibroblasts cells red with CellTracker CMRA and the whole spheroids blue with Hoechst 33342. As shown in **Fig. S15(C)**, the fibroblasts could well integrate with the tumor tissues. We believe that this spheroid model formed on this chip could offer a better choice for drug screening.

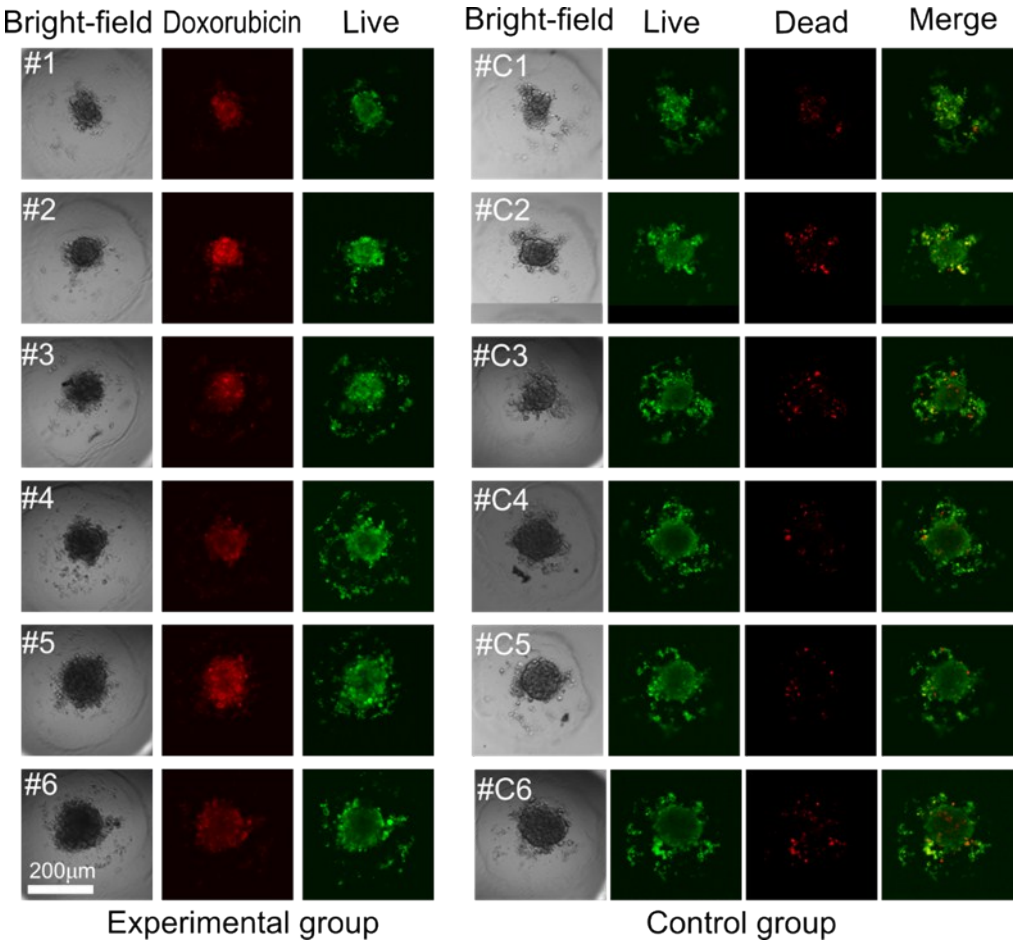

Fig. S16. The cell viability of mouse 4T1.2-fibroblast spheroids after the treatment with doxorubicin for 72h. The red fluorescence shows the distribution of DOX. Control group:

Live/dead test for the mouse 4T1.2-fibroblast spheroids. The green and red fluorescence indicate the live and dead cells in the spheroids, respectively.

To investigate the drug-resistance model for drug screening, we used the gradient-sized 4T1.2-fibroblast spheroids. It has been reported that the 4T1 tumor cells exhibit drug resistance to DOX in the reference[2]. The mouse 4T1.2 tumor spheroids were treated with the DOX in a concentration of 30 μg mL-1 for 3 days. We could see that the DOX could well penetrate the spheroids. The viability was tested. The results indicated that although the spheroids had been treated for 3 days by DOX, the cell viability was still as high as that of the control group. In addition, we believe that cell lines with drug resistance can also be used to form spheroids of different sizes using the platform presented in this work. It will help the researchers to study the mechanism underlying drug resistance.

Reference:

1 T. Nederman, B. Glimelius, B. Norling, J. Carlsson and U. Brunk, *Cancer Res.*, 1984, **44**, 3090–3097.

2 A. Bandyopadhyay, L. Wang, J. Agyin, Y. Tang, S. Lin, I. T. Yeh, K. De and L. Z. Sun, *PLoS One*, , DOI:10.1371/journal.pone.0010365.